Journal of Organometallic Chemistry 1001 (2023) 122869

Contents lists available at ScienceDirect

Journal of Organometallic Chemistry

journal homepage: www.elsevier.com/locate/jorganchem

A series of ferriostannylenes with differing terphenyl substituents

Alice C. Phung, James C. Fettinger, Philip P. Power *

Department of Chemistry, University of California, 1 Shields Avenue, Davis, CA 95616

ARTICLE INFO

Keywords:
Stannylene
Metallostannylene
Terphenyl
Tin
Iron
Bimetallic compound

ABSTRACT

A series of ferriostannylenes of formula $Ar^{Me6}SnFeCp(CO)_2$ (Ar^{Me6} = $-C_6H_3$-(C_6H_2–2,4,6-Me_3)$_2$, Cp = η^5-C_5H_5) (**1**), $Ar^{Me6}SnFeCp^*(CO)_2$ (Cp* = η^5-C_5Me_5) (**2**), and $Ar^{Me6}SnFeCp(CO)(PMe_3)$ (**3**) with differing iron and/or tin substituents was synthesized. Their structures and spectroscopic properties were examined by X-ray crystallography, NMR, IR, and UV–vis spectroscopy and compared with data for related species. The structural data showed that, as the size of the terphenyl substituent increases, the C-Sn-Fe angle decreases slightly which is contrary to steric expectations. The ^{1}H and ^{119}Sn NMR chemical shifts of the least crowded species **1** is similar to, but slightly upfield of those of its more hindered ferriostannylene analogs. Unexpectedly, **3** displayed a ^{119}Sn NMR chemical shift that is ca. 800 ppm downfield of **1** as a result of the substitution of one of the iron carbonyl groups with a PMe_3 ligand. This unusual finding is probably a reflection of a decreased paramagnetic shielding of the ^{119}Sn nucleus by the more electron releasing character of the PMe_3 ligand which decreases the n→p energy gap. The infrared spectrum of **1** also displayed slightly higher ν_{CO} frequencies, and its electronic spectrum indicated a small hypsochromic shift in the energy of its n→p transition whereas both **2** and **3** displayed much greater hypsochromic shifts than **1** consistent with the more electron donating character of the iron phosphine substituent. The results were interpreted in terms of the electronic/steric properties of the various substituents and their effects on metal electron density.

1. Introduction

Metallotetrylenes feature a two-coordinate heavy group 14 metal atom such as Si, [1] Ge, [2–8] Sn, [3,8–15] or Pb [14,16–18] with a direct σ bond to a transition metal moiety. The majority of known metallotetrylenes are metallostannylenes, and the transition metals are directly bonded to the tin atom are usually either members of group 6 (Cr, Mo, W) [8,9,13] or group 8 (Fe, Ru, Os) [3,10,12,14,15,19]. The metallotetrylene structures have bent coordination geometry at the tetrel atom, indicating the presence of a nonbonded lone pair and an unoccupied *p*-orbital. The related triple-bonded metallostanylynes, in which the coordination of Sn is linear or near-linear, are known to feature a triple bond to a tungsten [20,21] or molybdenum atom [22]. An exception is the chloride substituted manganostannylene ClSnMn $(CO)_3(CNAr^{iPr4})_2$ reported by Figueroa and coworkers featuring a σ bond between tin and manganese [11].

Most reports focus on the details of the synthesis and characterization of the metallostannylene, which usually involves the main group metal–transition metal bond formation via a salt metathesis route [3,9,14,15]. The metallostannylenes obtained were generally well-characterized by spectroscopic (^{1}H, ^{13}C, and ^{119}Sn NMR and electronic) and X-ray crystal diffraction data. Other routes to metallostannylenes include reactions involving isomerization, H migration, and halide or hydride abstraction (Fig. 1) [8,10,12,13,19]. The triple-bonded Sn≡W cationic complexes were produced by dinitrogen elimination [20,21] or chloride abstraction, [21] and the Sn≡Mo neutral complexes by metathetical exchange [22].

In addition to their syntheses, the reactivity of the metallotetrylenes has also been investigated [1,7,10,12,15,19,23–27]. However, there are few detailed investigations into how changing the substituents at the tetrel atom affects the spectroscopic properties of the complexes. Here, we report three new ferriostannylenes: $Ar^{Me6}SnFeCp(CO)_2$ (Ar^{Me6} = $-C_6H_3$-(C_6H_2–2,4,6-Me_3)$_2$, Cp = η^5-C_5H_5) (**1**), $Ar^{Me6}SnFeCp^*(CO)_2$ (Cp* = η^5-C_5Me_5) (**2**), and $Ar^{Me6}SnFeCp(CO)(PMe_3)$ (**3**).

2. Experimental section

2.1. General procedures

All manipulations were carried out by using modified Schlenk

* Corresponding author.
E-mail address: pppower@ucdavis.edu (P.P. Power).

https://doi.org/10.1016/j.jorganchem.2023.122869
Received 30 June 2023; Received in revised form 18 August 2023; Accepted 26 August 2023
Available online 7 September 2023

Salt metathesis.

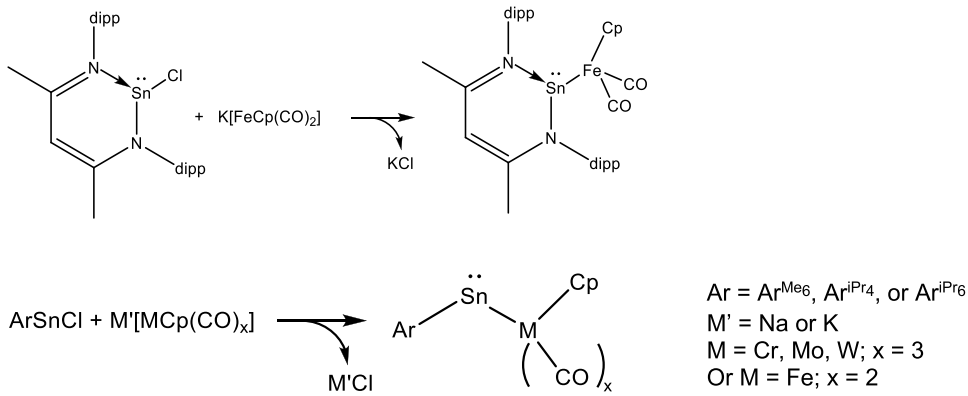

Deprotonation.

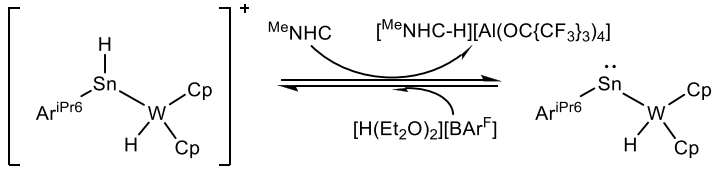

Isomerizaton/H-migration.

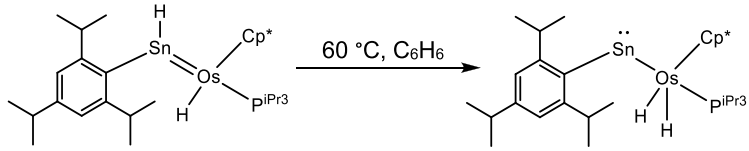

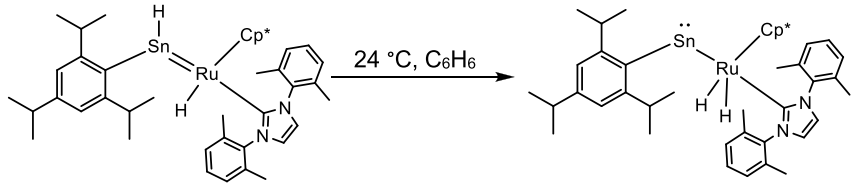

Chloride Abstraction.

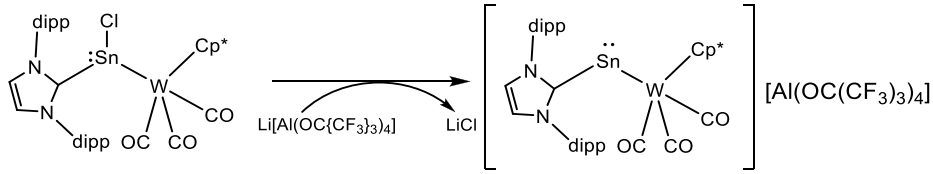

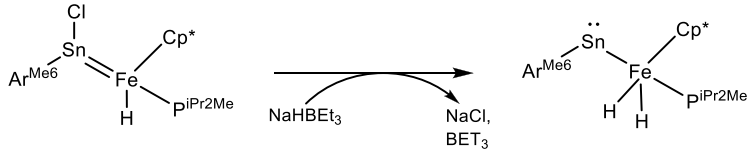

Fig. 1. Routes to metallostannylenes [3,8–10,12,13,15,19].

techniques or in a Vacuum Atmospheres OMNI-Lab drybox under a N_2 or argon atmosphere. Solvents were dried over columns of activated alumina using a Grubbs type purification system (Glass Contour), stored over Na (THF, toluene) or K (hexanes) mirrors, and degassed via three freeze-pump-thaw cycles prior to use. The ligand trimethylphosphine (PMe_3) was purchased from Strem Chemicals and transferred to a J. Young's Schlenk tube prior to use. The compounds $Ar^{Me6}SnCl$ [28–30] and $K[FeCp(CO)_2]$ [31] were synthesized according to literature procedures. The compound $K[FeCp^*(CO)_2]$ was synthesized by stirring a THF solution of $\{FeCp^*(CO)_2\}_2$ over a potassium mirror for 1 month. The ^1H and $^{13}C\{^1H\}$ NMR spectra were recorded on Varian 600 MHz NMR or Bruker 400 MHz NMR spectrometers and were referenced to the residual solvent signals in C_6D_6 (^1H: δ 7.15 ppm, ^{13}C: δ 128.06 ppm) [32]. The ^{31}P and ^{119}Sn NMR spectra were recorded on a Bruker Avance DRX 500 MHz spectrometer. UV–Visible spectra were recorded using dilute hexane solutions in 3.5 mL quartz cuvettes using an Olis 17 Modernized Cary 14 UV–Vis/NIR spectrophotometer. Infrared spectra for **1**–**3** were recorded as Nujol mulls between CsI windows on a PerkinElmer 1430 spectrophotometer. Melting points were determined in flame-sealed glass capillaries on a Meltemp II apparatus equipped with a partial immersion thermometer.

$Ar^{Me6}SnFeCp(CO)_2$ (1): A solution of $Ar^{Me6}SnCl$ [28–30] (3.5 g, 7.5 mmol) in THF (ca. 30 mL) was added dropwise to a THF suspension (ca. 40 mL) of $K[FeCp(CO)_2]$ [31] (1.6 g, 7.5 mmol) at ca. 0 °C with stirring. The dark red solution was allowed to slowly warm to room temperature and stirred until the solution became dark green, ca. 1–3 days. The solvent was removed under reduced pressure to afford a dark green-brown solid that was redissolved in toluene (ca. 50 mL). The toluene solution was filtered through a Celite/Florisil plug, and the deep green filtrate was concentrated to ca. 10 mL under reduced pressure. Storage at ca. -18 °C afforded dark green crystals of the product **1**. Yield: 4.6 g (50%). Mp: 280–285 °C. ^1H NMR (600 MHz, C_6D_6, 20 °C): δ 1.98 (s, 6H, *p*-C(C*H*$_3$)), δ 2.41 (s, 12H, *o*-C(C*H*$_3$)), δ 3.66 (s, 5H, η^5-C_5H_5), δ 6.65 (br s, 4H, flanking *m*-aromatic *H*), δ 7.16 (d, 2H, J_{HH} = 7.5 Hz, central m-aromatic *H*), δ 7.42 (t, 1H, $^3J_{HH}$ = 8.1 Hz, central *p*-aromatic *H*). $^{13}C\{^1H\}$ NMR (151 MHz, C_6D_6, 20 °C): δ 20.56 (*p*-*C*H$_3$) δ 20.97 (*o*-*C*H$_3$), δ 85.25 (η^5-*C*$_5$H$_5$), δ 127.13, 129.58, 136.78, 136.96, 145.59 (Ar(*C*)), δ 187.73 (C_{ipso}-Sn), δ 210.6 (*C*O). ^{119}Sn NMR (149 MHz, C_6D_6, 20 °C): δ 2957. UV–vis (hexane): λ_{max} (ε) 370 nm (4800 mol^{-1} L cm^{-1}), 594 nm (790 mol^{-1} L cm^{-1}). IR (Nujol, cm^{-1}): ν_{CO} 2010 (s), ν_{CO} 1950 (s).

$Ar^{Me6}SnFeCp^*(CO)_2$ (2): A solution of $Ar^{Me6}SnCl$ [28–30] (0.023 g, 0.051 mmol) in THF (15 mL) was added dropwise to a THF suspension (ca. 10 mL) of $K[FeCp^*(CO)_2]$ (0.014 g, 0.051 mmol) at -78 °C. The solution was allowed to warm slowly to room temperature and stirred until the solution was dark green, ca. 3 days. The solvent was removed under reduced pressure to afford a dark green solid that was dissolved in toluene (ca. 50 mL). This solution was filtered through a Celite plug, and the deep green filtrate was concentrated to ca. 10 mL. Storage at ca. -18 °C afforded dark green crystals of **2**. Yield: 0.022 g (60%). Mp: 270–275 °C. ^1H NMR: (500 MHz, C_7D_8, 20 °C) δ 1.38 (s, 15H, η^5-C_5(C*H*$_3$)$_5$), δ 2.08 (s, 6H, *p*-C(C*H*$_3$)), δ 2.56 (s, 12H, *o*-C(C*H*$_3$)), δ 6.75 (br s, 4H, flanking *m*-aromatic *H*), δ 7.16 (d, 2H, J_{HH} = 7.5 Hz, central m-aromatic *H*), δ 7.46 (t, 1H, $^3J_{HH}$ = 8.1 Hz, central *p*-aromatic *H*). UV–Vis (hexane): λ_{max} (ε) 384 nm (5500 mol^{-1} L cm^{-1}), λ_{max} (ε) 662 nm (0.2000 mol^{-1} L cm^{-1}). IR (Nujol, cm^{-1}): ν_{CO} 1990 (s), ν_{CO} 1945 (s).

$Ar^{Me6}SnFeCp(CO)(PMe_3)$ (3): Pure, undiluted trimethylphosphine PMe_3 (0.1 mL, 1 mmol) was added dropwise by cannula to a solution of **1** (0.6 g, 0.1 mmol, ca. 2 drops) in hexanes (ca. 40 mL) at ca. 0 °C, which was then allowed to slowly warm to room temperature, and stirred overnight. The resulting red solution was concentrated to ca. 20 mL under reduced pressure. Storage at ca. -18 °C gave purple crystals of **3**. Yield: 0.4 g (60%). Mp: 265–270 °C. ^1H NMR: (500 MHz, C_6D_6, 20 °C) δ 0.53 (d, 9H, $^2J_{HH}$ = 8.7 Hz, P(C*H*$_3$)$_3$), δ 1.99 (s, 6H, *o*-C(C*H*$_3$)), δ 2.46 (s, 6H, *o*-C(C*H*$_3$)), δ 2.61 (s, 6H, *p*-C(C*H*$_3$)), δ 3.61 (s, 5H, η^5-C_5H_5), δ 6.65 (s, 4H, flanking *m*-aromatic *H*), δ 7.13 (d, 2H, J_{HH} = 14.7 Hz, central m-aromatic *H*), δ 7.45 (t, 1H, $^3J_{HH}$ = 7.5 Hz, central *p*-aromatic *H*). ^{13}C NMR (151 MHz, C_6D_6, 20 °C): δ 20.33 (P(*C*H$_3$)$_3$), δ 20.56 (*p*-*C*H$_3$), δ 21.02 (*o*-*C*H$_3$), δ 21.97 (*o*-*C*H$_3$), δ 80.98 (η^5-*C*$_5$H$_5$), δ 127.66, 127.96, 128.16, 129.32, 136.36, 139.18 (Ar(*C*)), δ 166.86 (C_{ipso}-Sn), *C*O signal not observed. ^{31}P NMR (202 MHz, C_6D_6, 20 °C): δ 16.50. ^{119}Sn NMR (149 MHz, C_6D_6, 20 °C): δ 3762. UV–Vis (hexane): λ_{max} (ε) 350 nm (140 μmol^{-1} L cm^{-1}), λ_{max} (ε) 720 nm (1300 μmol^{-1} L cm^{-1}). IR (Nujol, cm^{-1}): ν_{CO} 1870 (s).

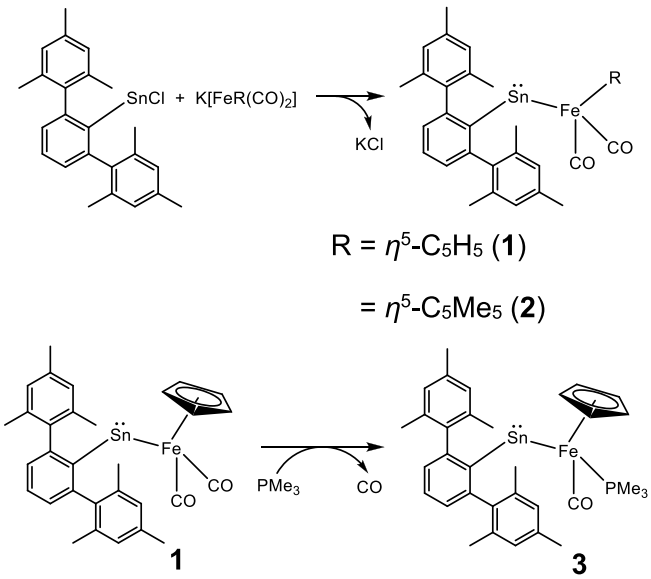

Scheme 1. Synthesis of compounds **1**–**3**.

3. Results and discussion

3.1. Synthesis

Compound **1** was synthesized via salt metathesis, similarly to the majority of reported metallostannylenes (Scheme 1) [3,9,14]. Treatment of 1 equiv of $Ar^{Me6}SnCl$ [28,30] with 1 equiv of $K[FeCp(CO)_2]$ [31] in THF gave a dark green solution from which crystals of the ferriostannylene $Ar^{Me6}SnFeCp(CO)_2$ (**1**) were obtained in moderate yield after workup and recrystallization from hexanes.

The synthesis of the potassium salt $K[FeCp^*(CO)_2]$ for use in the synthesis of **2** proved more difficult than its Cp substituted counterpart. A high-yield synthesis of $K[FeCp(CO)_2]$ was reported in 1981 by Plotkin and Shore and involves the use of the potassium ketyl radical to reduce the dimer $\{FeCp(CO)_2\}_2$ [31]. Unfortunately, a similar ketyl route proved ineffective for the reduction of the bulkier $\{FeCp^*(CO)_2\}_2$, and the unreduced dimer was recovered from the reaction mixture. Replacing the potassium ketyl with a sodium ketyl or KC_8 as reductants also proved ineffective. Ultimately, rapid stirring of 1 equiv of $\{FeCp^*(CO)_2\}_2$ over an excess of potassium in the form of a metal mirror gave, after washing with toluene, $K[FeCp^*(CO)_2]$ as a pink powder. However, this route proved to be very inefficient since it involved stirring over the potassium mirror for ca. 1 month which afforded a 3% yield of the potassium salt.

The synthesis of **2** proceeded similarly to that of **1**. Treatment of 1 equiv of the aryl stannylene chloride $Ar^{Me6}SnCl$ [28–30] with 1 equiv of the potassium salt $K[FeCp^*(CO)_2]$ gave green crystals of $Ar^{Me6}SnFeCp^*(CO)_2$ (**2**) in low yield after workup and crystallization from toluene. Due to the difficulty involving the long reaction time and low yield in producing the $[FeCp^*(CO)_2]^-$ anion, the quantity of pure crystals of **2** that were available were only sufficient for its characterization by ^1H NMR, UV–vis, IR spectroscopy, and X-ray crystallography. ^{13}C NMR and ^{119}Sn NMR spectra proved unobtainable due to the very low solubility of **2**.

The isolation of ferriostannylene **3** was achieved through a phosphine-carbonyl ligand substitution. Approximately 1 equiv of the volatile $PMe_3(l)$ was added dropwise via cannula to a stirred hexanes solution containing 1 equiv of **1**. Concentration of the green solution under reduced pressure of the hexanes solution gave purple-brown crystals of $Ar^{Me6}SnFeCp(CO)(PMe_3)$ (**3**) in moderate yield. Melting points of compounds **1–3** occur at high temperatures above 250 °C, with the cooled samples appearing brown to black in color, suggesting decomposition upon fusion.

NMR Spectroscopy. Comparison of the spectroscopic data for **1** to those of its more sterically crowded analogues $ArSnFeCp(CO)_2$ (Ar = Ar^{iPr4} or Ar^{iPr6}) [15] revealed some unexpected patterns. The ^{119}Sn NMR spectra of the ferriostannylenes $ArSnFeCp(CO)_2$ (Ar = Ar^{Me6} (**1**), δ = 2957 ppm; Ar = Ar^{iPr4}, δ = 2951 ppm; Ar = Ar^{iPr6}, δ = 2915 ppm) [15] indicate that the tin signal is shifted slightly upfield with increasing substituent size [32,33]. The apparent increase in shielding of the Sn by its substituents may be explained simply by inductive effects [34,35]. The ^{1}H NMR spectra show a gradual downfield shift of the cyclopentadienyl protons resonance, with the singlet appearing at 3.66 ppm in **1** (Ar = Ar^{Me6}), at 3.78 ppm in $Ar^{iPr4}SnFeCp(CO)_2$ and at 3.80 ppm in $Ar^{iPr6}SnFeCp(CO)_2$ [15]. The decreased shielding of the Cp group on the iron moiety can be attributed to an increased ionic character of the Fe–Cp bond in association with the increased π*-backbonding from the strong-field CO groups illustrated in the IR spectra (vide infra).

Compounds **1** and **2** differ only in their Cp and Cp* ligand. An overlay of the ^{1}H NMR spectra of compounds **1** and **2** indicates a small downfield shift of the protons on the flanking phenyl rings of the terphenyl ligand in **2** while chemical shifts of the terphenyl ligand protons oriented away from the Cp ring remain unchanged. The deshielding of the ligand protons in closest proximity to the Cp* group in **2** is also observed in the mesitylene protons of the metallogermylenes Mes*GeFe$(CO)_2$R (R = Cp or Cp*) (Mes* = C_6H_2–2,4,6-$^tBu_3$) [36].

The signals corresponding to the terphenyl *o*-methyl group in both the ^{1}H (2.41 ppm) and ^{13}C (20.97 ppm) NMR spectra of **1** are split into two singlets of equal intensity in the respective spectra for **3** (^{1}H: 2.46 and 2.61 ppm; ^{13}C: 21.02 and 21.97 ppm), consistent with a lower symmetry arising from the phosphine-carbonyl ligand substitution. Moreover, the PMe_3 protons in **3** appear in the ^{1}H NMR spectrum as a doublet at 0.53 ppm as a due to coupling to the ^{31}P nucleus.

The ^{31}P NMR signal of **3** appears at 16.50 ppm Other organophosphine-substituted metallostannylenes feature a ^{31}P NMR signal shift in the range 41.16 – 76.2 ppm, [10,14,19] and. as other phosphine-containing metallostannylenes feature P^iPr_3 [10] or PMe^iPr_2, [14,19]. The downfield shifted signal of **3** can be partly attributed to the smaller size of PMe_3. Generally speaking, decreased steric congestion at the phosphorus atom has been shown to result in shorter metal-phosphorus bond lengths and a more shielded phosphorus nucleus [37–43].

The published ^{119}Sn NMR chemical shifts of metallostannylenes feature a signal in the range 1982 – 2951 ppm, [9,15,19,32]. The ^{119}Sn chemical shifts of **1** and **2** lie within this range. However the chemical shift of **3** lies much further downfield at 3762 ppm. This may be attributed a change in paramagnetic shielding of the tin nucleus which is a reflection of the mixing of the ground and excited states of the tin center [44]. This is increased (shifting the resonance downfield, i.e. opposite of the inductive effect) by the more electron donating PMe_3 ligand in **3**. This correlates with a the lower n-p energy gap (see also next section) in comparison to ferriostannylenes **1**, and **2**.

UV–vis and IR Spectroscopy. Solutions of **3** are dark yellow to brown in color, in contrast to the typical dark green solutions shown by ferriostannylenes **1, 2**, and the more crowded species $ArSnFeCp(CO)_2$ (Ar = Ar^{iPr4} or Ar^{iPr6}) [15]. The UV–vis spectrum of **1** and **2** has similarities to those of the other ferriostannylenes, displaying a relatively intense band in the near UV region (below 400 nm) and a less intense band in the visible region at 598 nm (**1**), and 662 nm (**2**) [45]. The bands in the visible region correspond to an n→p transition and the greater bathochromic shift displayed by **2** may be partly explained by the narrowing of the bending angle at Sn as seen in its X-ray crystal structure. The n→p band energy value can display a relationship with the interligand angles but such a correlation is not observed the diaryl stannylenes $SnAr_2$ (Ar = Ar^{Me6}, Ar^{iPr4}, or Ar^{iPr6}) where the bending angles are also complicated by dispersion energies [46].

Table 1
Selected spectroscopic data for $ArSnFeCp(CO)_2$ (Ar = Ar^{iPr4} or Ar^{iPr6})[15] and **1–3**.

	$Ar^{iPr6}SnFeCp(CO)_2$ [15]	$Ar^{iPr4}SnFeCp(CO)_2$ [15]	1	2	3
C-Sn-Fe, (deg)	106.6(2)	112.65(9)	113.60 (3)	111.05 (15)	114.3 (12) 116.88 (9)
^{1}H NMR: $\delta_{Cp\ H}$ (ppm)	3.80	3.78	3.66	–	3.61
^{119}Sn: (ppm)	2915	2951	2957	–	3762
IR: νCO (cm^{-1})	1967 1926	1970 1921	2010 1950	1990 1945	1870
UV–vis: λ_{max} (n→p transition, nm)	608	608	598	662	720

The structural and spectroscopic data for ferriostannylenes **1, 2** and $ArSnFeCp(CO)_2$ (Ar = Ar^{iPr4} or Ar^{iPr6}), (Table 1) provide little evidence of any strong structural/spectroscopic data correlation. Although, the UV–vis absorptions for $Ar^{iPr4}SnFeCp(CO)_2$ and $Ar^{iPr6}SnFeCp(CO)_2$ are essentially identical [15], despite the narrower bending angle of 106.6 (2)° at tin [15]. The larger terphenyl ligand, Ar^{iPr6}, appears to decrease the angle possibly as a result of London Dispersion interactions between the more numerous C—H ligand substituents in that ligand. But apparently this has little or no effect on the UV–vis spectrum. The X-ray crystal structure for **3** shows a wider C-Sn-Fe bond angle than that of **1**, and if earlier patterns are followed, there should be a hypsochromic shift in the n→p transition of **3**. However, this absorption for **3** occurs at a markedly higher wavelength outside the 569 – 620 nm range in the other metallostannylenes [9,15]. This is consistent with the lowering of the energy of the HOMO-LUMO as proposed as the cause of the larger downfield chemical shift of the ^{119}Sn NMR signal as discussed above.

IR Spectroscopy. The IR spectrum of $ArSnFeCp(CO)_2$ show that the CO stretching bands shift to lower wavenumbers as the alkyl substituent size increases: from 2010 to 1950 cm^{-1} in **1**, to 1970 and 1921 cm^{-1} when Ar = Ar^{iPr4}, and 1967 and 1926 cm^{-1} when Ar = Ar^{iPr6} [15]. The shift to lower frequencies suggests an increase in π*-backbonding and a corresponding strengthening of the Fe–C bonds [45].

The IR spectrum of **2** displays carbonyl stretching bands shifted to lower frequencies in comparison to **1** at 1990 and 1945 cm^{-1}. This difference is paralleled to an even greater extent in the

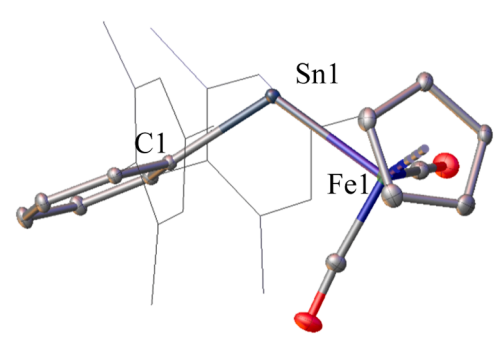

Fig. 2. Thermal ellipsoid plot (50%) of **1**. Carbon-bound H atoms are not shown and flanking phenyl rings are shown as wire frames for clarity. Selected bond lengths (Å) and angles (deg): Sn1–C1 = 2.2101(11); Sn1–Fe1 = 2.5854 (3); C1–Sn1–Fe1 = 113.60(3)°.

Table 2
Selected structural data for **1–3**.

	$Ar^{iPr6}SnFeCp(CO)_2$ [15]	$Ar^{iPr4}SnFeCp(CO)_2$ [15]	1	2	3
C_{ipso}–Sn, Å	2.444(7)	2.209(3)	2.2101 (11)	2.088 (5)	2.226 (3)
Sn–Fe, Å	2.6031(17)	2.5633(6)	2.5854 (3)	2.5609 (11)	2.561 (4) 2.5562 (8)
Fe–$Cp_{centroid}$, Å	1.577(6)	1.671(6) 1.706(3)	1.7373 (4)	1.738 (3)	1.732 (2) 1.729 (10)
Fe–CO, Å	1.930(17) 1.739(10)	1.749(6) 1.732(4) 1.755(13)	1.767 (3) 1.750 (3)	1.766 (8) 1.739 (8)	1.730 (6) 1.73 (3)
C_{ipso}–Sn–Fe, deg	106.67(19)	112.65(9)	113.60 (3)	111.05 (15)	114.32 (12) 116.88 (9)
Fe–PMe_3, Å	–	–	–	–	2.1555 (9) 2.1709 (13)

metallogermylenes Mes*GeFe(CO)$_2$R by the ν_{CO} bands at 2004 and 1950 cm^{-1} (R = Cp) to 1969 and 1920 cm^{-1} (R = Cp*) [36]. The inductive effects of the methyl groups [34,35] cause an increase in electron density at the transition metal that is reflected in the strengthened Fe–C bond.

The IR spectrum of **3** displays a single CO stretching band at 1870 cm^{-1}, which appears at a lower wavenumber in comparison to the ν_{CO} of **1**, **2**, and ArSnFeCp(CO)$_2$ (Ar = Ar^{iPr4} or Ar^{iPr6}) [15]. Given the weaker π-acceptor ability of PMe_3 in comparison to CO, [45] the lower frequency observed for **3** indicates that the single CO group bears the majority of the π*-backdonation and contributes to a relatively stronger Fe–C bond than the other ferriostannylenes.

3.2. X-ray crystal structures

The ferriostannylene **1** crystallizes from toluene as green blocks in the monoclinic space group $P2_1/c$ that have identical values to those of its Ge congener $Ar^{Me6}GeFeCp(CO)_2$ [24]. The structure of **1** (Fig. 2.) features a C_{ipso}-Sn-Fe bending angle of 113.60(3)°, which is within the range of other neutral metallostannylenes (106.1(3)° – 118.76(5)°) [8,9,12–14,19].. With the exception of the red and dichroic polymorphs of the corresponding ferriogermylene, the interligand angle at the tetrel atom in tetrylenes has generally been observed to be wider in the Ge complexes compared to the Sn congeners [15,29,47].

Compound **1** contains the least sterically encumbering ligand of the three ferriostannylenes and a comparison the C_{ipso}-Sn-Fe angles of the three ferriostannylenes reveals a decreasing interligand angle with increasing terphenyl size (Ar^{Me6} (**1**) = 113.60(3)°, Ar^{iPr4} = 112.65(9)°, Ar^{iPr6} = 106.6(2)°) [15] (Table 2). This sterically counterintuitive trend was previously observed in the interligand angles of the diaryl stannylenes:$SnAr_2$ (Ar = Ar^{Me6}: 114.7(2)°, Ar^{iPr4}: 117.56(8)°, Ar^{iPr6}: 107.61 (9)°) [29,45,47,48] and was shown to be due to London dispersion effects from the H···H attraction between the terphenyl ligands [47,48]. The X-ray crystal structures of the ferriostannylenes show that the Cp or Cp* ring is oriented towards one of the flanking phenyl rings, further supporting the view that London dispersion effects play a role in determining the interligand angle of the ferriostannylenes (Fig. 3**a**). X-ray crystal structures of the metallotetrylenes $Ar^{iPr6}SnMCp(CO)_3$ (M = Cr, Mo, W) [9] similarly show the cyclopentadienyl fragment oriented towards the large aryl ligand rather than away from it. The structures of the three ferriostannylenes show that the closest H···H distances between the alkyl substituent protons on the ligand and Cp ring protons are 3.20245(13) Å in **1**, 2.41579(12) Å in $Ar^{iPr4}SnFeCp(CO)_2$ (Fig. 3**b**), and 2.8503(2) in $Ar^{iPr6}SnFeCp(CO)_2$.

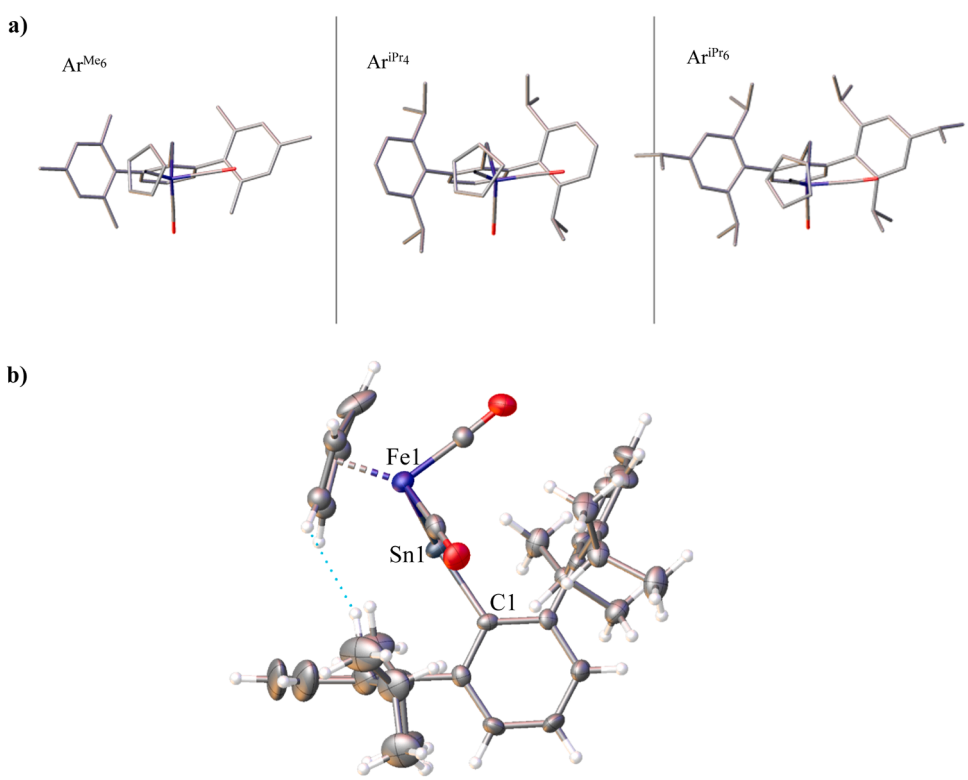

Fig. 3. a) Molecular graphics of **1** (left), $Ar^{iPr4}SnFeCp(CO)_2$ (center), and $Ar^{iPr6}SnFeCp(CO)_2$ (right) in the "tube" drawing, showing the Cp fragment oriented towards the flanking phenyl ring. **b)** Thermal ellipsoid plot (50%) of $Ar^{iPr}_4SnFeCp(CO)_2$ showing the H···H contact (2.41579(12) Å).

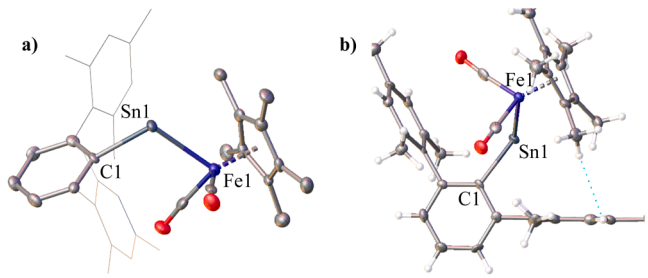

Fig. 4. Thermal ellipsoid plots (50%) of **2. a)** "Side" view of **2**. Carbon-bound H atoms are not shown, and flanking phenyl rings are shown as wire frames for clarity. **b)** Rotated view of **2** showing the H···H contact (2.6909(3) Å). Selected bond lengths (Å) and angles (deg): Sn1–C1 = 2.088(5); Sn1–Fe1 = 2.5609(11); C1–Sn1–Fe1 = 111.05(15)°.

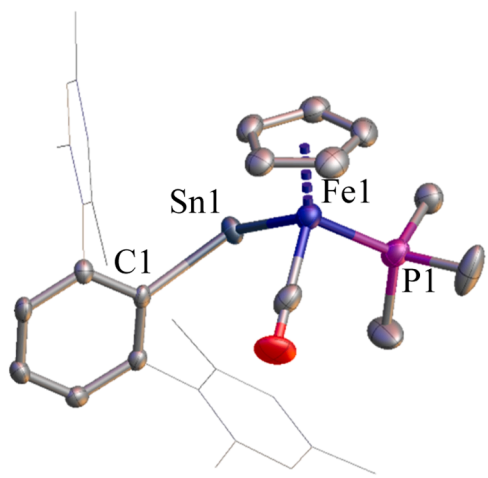

Fig. 5. Thermal ellipsoid plot (50%) of **3**. Carbon-bound H atoms and structural disorder are not shown, Mesityl rings are in wire frame. Selected bond lengths (Å) and angles (deg): Sn1–C1 = 2.226(3); Sn1–Fe1 = 2.561(4), 2.5562 (8); C1–Sn1–Fe1 = 114.3(12)°.

The ferriostannylene **2** (Fig. 4.) crystallizes as green blocks in the triclinic space group $P\bar{1}$. In comparison to **1**, compound **2** differs in its slightly narrower C_{ipso}-Sn-Fe bond angle (Table 1). Though Cp* is a more electron-rich group than Cp, [45] the Sn–Fe and Fe–$Cp^*_{centroid}$ distances remain similar to those of **1**, suggesting that attractive dispersion effects between the methyl substituents are significant. Unlike **1** and **2**, the molybdostannylene pair $Ar^{iPr6}SnMo(\eta^5\text{-}C_5H_5)(CO)_3$ and $Ar^{iPr6}SnMo(\eta^5\text{–}1,3\text{-}Bu^t_2\text{-}C_5H_3)(CO)_3$ show that the interligand angle at tin increases from 110.14(10)° to 112.10(8)° as the number of Cp methyl substituents increases [9]. Additionally, the structure of $Ar^{iPr6}SnMo(\eta^5\text{–}1,3\text{-}Bu^t_2\text{-}C_5H_3)(CO)_3$ shows that the two *tert*-butyl groups are oriented away from the terphenyl ligand, [9] which suggests that despite the larger alkyl substituents on the Cp ring, reducing steric crowding takes precedence over increasing dispersion effects.

Compound **3** (Fig. 5.) crystallizes as purple blocks in the triclinic space group $P\bar{1}$. The {FeCp(CO)(PMe_3)} fragment is disordered over two sites. The Fe–CO (1.730(6) and 1.73(3) Å) and Fe–PMe_3 (2.1555(9) and 2.1709(13) Å) bond distances are shorter than the sum of the covalent radii of Fe (1.16 Å), C (0.75 Å), and P (1.11 Å), [49] supporting the IR and ^{31}P NMR spectra which are consistent with increased backbonding into the π* orbital of CO and σ* orbital of PMe_3. The C_{ipso}-Sn-Fe bond angles in **3** are the widest of the three ferriostannylenes, at 114.3(12)° and 116.88(9)°. In general, metallostannylenes containing an organophosphine at the transition metal atom display a larger interligand angle at tin. For example, $Ar^{Me6}SnRuCp^*(H)_2(PMe^iPr_2)$ and $Ar^{Me6}SnFeCp^*(H)_2(PMe^iPr_2)$ feature angles at the upper limits of the C_{ipso}-Sn-M range (106.1(3)° – 118.76(5)°) [8,9,12–14,19] at 117.98(10) and 118.76(5), respectively [14,19]. Compound **3** has a narrower interligand angle than those metallostannylenes likely due to the smaller organophosphine PMe_3 substituent in comparison to the PMe^iPr_2 ligand [14,19]. Both the crystal structures of $Ar^{Me6}SnRuCp^*(H)_2(PMe^iPr_2)$ and $Ar^{Me6}SnFeCp^*(H)_2(P^iPr_2Me)$ show the isopropyl substituents on the phosphorus atom oriented away from the terphenyl ligand, consistent with the more important role of steric effects in the metallostannylene structure.

4. Conclusion

Three ferriostannylenes with different terphenyl tin aryl and iron substituents were synthesized. Comparisons of their spectroscopic and structural properties reveal changes that indicate increased stability arising from attractive dispersion C···H interactions. Complex **2** differs from **1** in that a methyl-substituted cyclopentadienyl group replaces the original Cp ligand. This has a similar effect to that of increasing the substituent bulk on the terphenyl ligands. Overall, a larger substituent bulk at the aryl groups results in a counterintuitive narrower angle at tin which yields a lower-energy n→p transition. Complex **3** differs from **1** via replacement of a CO with which PMe_3 yields a wider interligand the angle at the Sn center and a much larger downfield shift of its ^{119}Sn NMR chemical shift.

Accession codes

CCDC 2258106 – 2258108 contain the supplementary crystallographic data for this paper. These data can be obtained free of charge via www.ccdc.cam.ac.uk/data_request/cif, or by emailing data_request@ccdc.cam.ac.uk, or by contacting The Cambridge Crystallographic Data Centre, 12 Union Road, Cambridge CB2 1EZ, UK; fax: +44 1223 336033.

Author contributions

The manuscript was written through contributions of all authors. All authors have given approval to the final version of the manuscript.

Declaration of Competing Interest

The authors declare no competing financial interest.

Data availability

Data will be made available on request.

Funding sources

U.S. National Science Foundation (CHE-2152760)
X-ray diffractometer (NSF Grant 0840444)

Acknowledgement

We thank the U.S. National Science Foundation for financial support (CHE-2152760) and the X-ray diffractometer (Grant 0840444).

Supplementary materials

Supplementary material associated with this article can be found, in the online version, at doi:10.1016/j.jorganchem.2023.122869.

References

[1] H.-J. Liu, C. Landis, C. Raynaud, O. Eisenstein, T.D. Tilley, Donor-promoted 1,2-hydrogen migration from silicon to a saturated ruthenium center and access to

silaoxiranyl and silaiminyl complexes, J. Am. Chem. Soc. 137 (2015) 9186–9194, https://doi.org/10.1021/jacs.5b05571.

[2] L. Pu, B. Twamley, S.T. Haubrich, M.M. Olmstead, B.V. Mork, R.S. Simons, P. P. Power, Triple bonding to germanium: characterization of the transition metal germylynes (η^5-C_5H_5)(CO)$_2$M⋮Ge-C_6H_3-2,6-Mes_2 (M = Mo, W; Mes = −C_6H_2-2,4,6-Me_3) and (η^5-C_5H_5)(CO)$_2$M⋮Ge-C_6H_3-2,6-$Trip_2$ (M = Cr, Mo, W; Trip = −C_6H_2-2,4,6-i-Pr_3) and the related single bonded metallogermylenes (η^5-C_5H_5)(CO)$_3$M-Ge-C_6H_3-2,6-$Trip_2$ (M = Cr, W), J Am Chem Soc. 122 (2000) 650–656.

[3] S. Inoue, M. Driess, Isolable metallo-germylene and metallo-stannylene σ-complexes with iron, Organometallics 28 (2009) 5032–5035, https://doi.org/10.1021/om9005802.

[4] W.-P. Leung, W.-K. Chiu, T.C.W. Mak, Synthesis and structural characterization of metallogermylenes, Cp-substituted germylene, and a germanium(II)-borane adduct from pyridyl-1-azaallyl germanium(II) chloride, Organometallics 31 (2012) 6966–6971, https://doi.org/10.1021/om3007739.

[5] S. Tashita, T. Watanabe, H. Tobita, Synthesis of a base-stabilized (chlorogermyl) metallogermylene and its photochemical conversion to a (Chlorogermyl)germylyne complex, Chem. Lett. 42 (2013) 43–44, https://doi.org/10.1246/cl.2013.43.

[6] K. Inomata, T. Watanabe, H. Tobita, Cationic metallogermylene and dicationic dimetallodigermenes: synthesis by chloride abstraction from *N*-heterocyclic carbene-stabilized chlorometallogermylenes, J. Am. Chem. Soc. 136 (2014) 14341–14344, https://doi.org/10.1021/ja506018f.

[7] K. Inomata, T. Watanabe, Y. Miyazaki, H. Tobita, Insertion of a cationic metallogermylene into E–H bonds (E = H, B, Si), J. Am. Chem. Soc. 137 (2015) 11935–11937, https://doi.org/10.1021/jacs.5b08169.

[8] M. Widemann, S. Jeggle, M. Auer, K. Eichele, H. Schubert, C.P. Sindlinger, L. Wesemann, Hydridotetrylene [Ar*EH] (E = Ge, Sn, Pb) coordination at tantalum, tungsten, and zirconium, Chem. Sci. 13 (2022) 3999–4009, https://doi.org/10.1039/D2SC00297C.

[9] B.E. Eichler, A.D. Phillips, S.T. Haubrich, B.V. Mork, P.P. Power, Synthesis, structures, and spectroscopy of the metallostannylenes (η^5-C_5H_5)(CO)$_3$M−Sn−C_6H_3-2,6-Ar_2 (M = Cr, Mo, W; Ar = C_6H_2-2,4,6-Me_3, C_6H_2-2,4,6-Pr^i_3), Organometallics 21 (2002) 5622–5627, https://doi.org/10.1021/om020583g.

[10] P.G. Hayes, C.W. Gribble, R. Waterman, T.D. Tilley, A hydrogen-substituted osmium stannylene complex: isomerization to a metallostannylene complex via an unusual α-hydrogen migration from tin to osmium, J. Am. Chem. Soc. 131 (2009) 4606–4607, https://doi.org/10.1021/ja901050m.

[11] M.A. Stewart, C.E. Moore, T.B. Ditri, L.A. Labios, A.L. Rheingold, J.S. Figueroa, Electrophilic functionalization of well-behaved manganese monoanions supported by m-terphenyl isocyanides, Chem. Commun. 47 (2011) 406–408, https://doi.org/10.1039/C0CC02742A.

[12] H.-J. Liu, J. Guihaumé, T. Davin, C. Raynaud, O. Eisenstein, T.D. Tilley, 1,2-Hydrogen migration to a saturated ruthenium complex via reversal of electronic properties for tin in a stannylene-to-metallostannylene conversion, J. Am. Chem. Soc. 136 (2014) 13991–13994, https://doi.org/10.1021/ja507799e.

[13] Y.N. Lebedev, U. Das, G. Schnakenburg, A.C. Filippou, Coordination chemistry of $[E(Idipp)]^{2+}$ ligands (E = Ge, Sn): metal germylidyne $[Cp^*(CO)_2W{\equiv}Ge(Idipp)]^+$ and metallotetrylene $[Cp^*(CO)_3W–E(Idipp)]^+$ cations, Organometallics 36 (2017) 1530–1540, https://doi.org/10.1021/acs.organomet.7b00110.

[14] P.W. Smith, R.C. Handford, T.D. Tilley, Heavy tetrel complexes of Ru featuring Ru=E(R)X and Ru–E–R (E = Sn, Pb) linkages, Organometallics 38 (2019) 4060–4065, https://doi.org/10.1021/acs.organomet.9b00550.

[15] H. Lei, J.-D. Guo, J.C. Fettinger, S. Nagase, P.P. Power, Synthesis, characterization, and CO elimination of ferrio-substituted two-coordinate germylenes and stannylenes, Organometallics 30 (2011) 6316–6322, https://doi.org/10.1021/om200912x.

[16] Q. Zhu, J.C. Fettinger, P. Vasko, P.P. Power, Interactions of a diplumbyne with dinuclear transition metal carbonyls to afford metalloplumbylenes, Organometallics 39 (2020) 4629–4636, https://doi.org/10.1021/acs.organomet.0c00659.

[17] N. Seidel, K. Jacob, A.K. Fischer, Bis[2-((dimethylamino)methyl)ferrocenyl]lead, (FcN)2Pb, as a ligand: synthesis and characterization of the heterotrimetallic metalloplumbylene compounds $(FcN)_2PbM(CO)_5$ (M = Cr, Mo, W), Organometallics 20 (2001) 578–581, https://doi.org/10.1021/om000796a.

[18] L. Pu, P.P. Power, I. Boltes, R. Herbst-Irmer, Synthesis and characterization of the metalloplumbylenes (η^5-C_5H_5)(CO)$_3$M-Pb-C_6H_3-2,6-$Trip_2$ (M = Cr, Mo, or W; Trip = −C_6H_2-2,4,6-i-Pr_3), Organometallics 19 (2000) 352–356, https://doi.org/10.1021/om990774s.

[19] R.C. Handford, M.A. Nesbit, P.W. Smith, R.D. Britt, T.D. Tilley, Versatile Fe–Sn bonding interactions in a metallostannylene system: multiple bonding and C–H bond activation, J. Am. Chem. Soc. 144 (2022) 358–367, https://doi.org/10.1021/jacs.1c10144.

[20] A.C. Filippou, P. Portius, A.I. Philippopoulos, H. Rohde, Triple bonding to tin: synthesis and characterization of the stannylyne complex trans-[Cl(PMe_3)$_4$W≡Sn-C_6H_3-2,6-Mes_2], Angew. Chem. Int. Ed. 42 (2003) 445–447, https://doi.org/10.1002/anie.200390135.

[21] A.C. Filippou, A.I. Philippopoulos, G. Schnakenburg, Triple bonding to tin: synthesis and characterization of the square-pyramidal stannylyne complex cation $[(dppe)_2W{:}Sn{-}C_6H_3\text{-}2,6\text{-}Mes_2]^+$ (dppe = $Ph_2PCH_2CH_2PPh_2$, Mes = C_6H_2-2,4,6-Me_3), Organometallics 22 (2003) 3339–3341, https://doi.org/10.1021/om030303c.

[22] J.D. Queen, A.C. Phung, C.A. Caputo, J.C. Fettinger, P.P. Power, Metathetical exchange between metal–metal triple bonds, J. Am. Chem. Soc. 142 (2020) 2233–2237, https://doi.org/10.1021/jacs.9b13604.

[23] A. El-Maradny, H. Tobita, H. Ogino, Photoreactions of silyliron(II) complexes Cp′Fe(CO)$_2$SiMe$_3$ (Cp′ = η^5-C_5H_5, η^5-C_5Me_5) with Di-*p*-tolylgermane (*p*-Tol)$_2$GeH$_2$, Chem Lett. 25 (1996) 83–84, https://doi.org/10.1246/cl.1996.83.

[24] A.C. Phung, J.C. Fettinger, P.P. Power, Insertion reactions of NH_3 and H_2O with the ferriogermylenes ArGeFeCp(CO)$_2$ (Ar = Ar^{Me6} (−C_6H_3-(C_6H_2-2,4,6-Me_3)$_2$) or Ar^{iPr4} (−C_6H_3-(C_6H_3-2,6-$^iPr_2$)$_2$); Cp = η^5-C_5H_5): structural isomerism and polymorphism in a metallogermylene, Organometallics 40 (2021) 3472–3479, https://doi.org/10.1021/acs.organomet.1c00475.

[25] A.C. Filippou, O. Chernov, G. Schnakenburg, Metal-silicon triple bonds: nucleophilic addition and redox reactions of the silylidyne complex [Cp(CO)2Mo≡Si-R], Angew. Chem. Int. Ed. 50 (2011) 1122–1126, https://doi.org/10.1002/anie.201005794.

[26] M.L. bin Ismail, F.-Q. Liu, W.-L. Yim, R. Ganguly, Y. Li, C.-W. So, Reactivity of a base-stabilized germanium(I) dimer toward group 9 metal(I) chloride and dimanganese decacarbonyl, Inorg. Chem. 56 (2017) 5402–5410, https://doi.org/10.1021/acs.inorgchem.7b00503.

[27] H.-J. Liu, M.S. Ziegler, T.D. Tilley, The Ruthenostannylene Complex [Cp*(IXy)H_2Ru-Sn-Trip]: providing access to unusual Ru-Sn bonded Stanna-imine, stannene, and ketenylstannyl complexes, Angewandte Chemie International Edition. 54 (2015) 6622–6626, https://doi.org/10.1002/anie.201502156.

[28] K. Ruhlandt-Senge, J.J. Ellison, R.J. Wehmschulte, F. Pauer, P.P. Power, Isolation and structural characterization of unsolvated lithium aryls, J. Am. Chem. Soc. 115 (1993) 11353–11357, https://doi.org/10.1021/ja00077a038.

[29] R.S. Simons, L. Pu, M.M. Olmstead, P.P. Power, Synthesis and characterization of the monomeric diaryls M{C_6H_3-2,6-Mes_2}$_2$ (M = Ge, Sn, or Pb; Mes = 2,4,6-$Me_3C_6H_2$−) and dimeric aryl−metal chlorides [M(Cl){C_6H_3-2,6-Mes_2}]$_2$ (M = Ge or Sn), Organometallics 16 (1997) 1920–1925, https://doi.org/10.1021/om960929l.

[30] L. Pu, M.M. Olmstead, P.P. Power, B. Schiemenz, Synthesis and characterization of the monomeric terphenyl−metal halides Ge(Cl){C_6H_3-2,6-$Trip_2$} (Trip = C_6H_2-2,4,6-*i*-Pr_3) and Sn(I){C_6H_3-2,6-$Trip_2$} and the terphenyl−metal amide Sn{N($SiMe_3$)$_2$}{C_6H_3-2,6-$Trip_2$}, Organometallics 17 (1998) 5602–5606, https://doi.org/10.1021/om980697l.

[31] J.S. Plotkin, S.G. Shore, Convenient preparation and isolation of pure potassium cyclopentadienyldicarbonylferrate, K[(η^5-C_5H_5)Fe(CO)$_2$], Inorg. Chem. 20 (1981) 284–285, https://doi.org/10.1021/ic50215a060.

[32] G.R. Fulmer, A.J.M. Miller, N.H. Sherden, H.E. Gottlieb, A. Nudelman, B.M. Stoltz, J.E. Bercaw, K.I. Goldberg, NMR chemical shifts of trace impurities: common laboratory solvents, organics, and gases in deuterated solvents relevant to the organometallic chemist, Organometallics 29 (2010) 2176–2179, https://doi.org/10.1021/om100106e.

[33] B. Wrackmeyer, 119Sn-NMR parameters, in: 1985: pp. 73–186. https://doi.org/10.1016/S0066-4103(08)60226-4.

[34] L.M. Stock, The origin of the inductive effect, J. Chem. Educ. 49 (1972) 400, https://doi.org/10.1021/ed049p400.

[35] W.M. Schubert, R.B. Murphy, J. Robins, Electron donor and acceptor properties of alkyl substituents, Tetrahedron 17 (1962) 199–214, https://doi.org/10.1016/S0040-4020(01)99020-9.

[36] P. Jutzi, C. Leue, (Supermesityl)chlorogermylene (Supermesityl = Mes* = 2,4,6-$^tBu_3C_6H_2$): synthesis and derivatization to (supermesityl)ferriogermylenes, Organometallics 13 (1994) 2898–2899, https://doi.org/10.1021/om00019a054.

[37] B.L. Shaw, Some steric, conformational and entropy effects of tertiary phosphine ligands, J. Organomet. Chem. 200 (1980) 307–318, https://doi.org/10.1016/S0022-328X(00)88652-0.

[38] S. Xiao, W.C. Trogler, D.E. Ellis, Z. Berkovitch-Yellin, Nature of the frontier orbitals in phosphine, trimethylphosphine, and trifluorophosphine, J. Am. Chem. Soc. 105 (1983) 7033–7037, https://doi.org/10.1021/ja00362a004.

[39] C.A. Tolman, Steric effects of phosphorus ligands in organometallic chemistry and homogeneous catalysis, Chem. Rev. 77 (1977) 313–348, https://doi.org/10.1021/cr60307a002.

[40] S.P. Wang, M.G. Richmond, M. Schwartz, NMR evidence for the existence of a π-accepting PMe_3 ligand. Estimates of the magnitude of π effects of WL(CO)$_5$ complexes, J. Am. Chem. Soc. 114 (1992) 7595–7596, https://doi.org/10.1021/ja00045a061.

[41] S.T. Krueger, R. Poli, A.L. Rheingold, D.L. Staley, Synthesis, molecular and electronic structure, and properties of mononuclear trimethylphosphine-containing cyclopentadienyl derivatives of molybdenum(III) and molybdenum(IV). Direct evidence of molybdenum(III)-phosphorus π back-bonding, Inorg. Chem. 28 (1989) 4599–4607, https://doi.org/10.1021/ic00325a013.

[42] S. Song, E.C. Alyea, Steric effects of bulky phosphines on ^{95}Mo NMR shieldings, Can. J. Chem. 74 (1996) 2304–2320, https://doi.org/10.1139/v96-258.

[43] R. Bosque, J. Sales, A QSPR study of the ^{31}P NMR chemical shifts of phosphines, J. Chem. Inf. Comput. Sci. 41 (2001) 225–232, https://doi.org/10.1021/ci000458k.

[44] B.E. Eichler, B.L. Phillips, P.P. Power, M.P. Augustine, Solid state and high resolution liquid ^{119}Sn NMR spectroscopy of some monomeric two-coordinate low-valent tin compounds: very large chemical shift anisotropies, Inorg. Chem. 39 (2000) 5450–5453, https://doi.org/10.1021/ic000514z.

[45] R.H. Crabtree, Carbonyls, phosphines, and substitution. The Organometallic Chemistry of the Transition Metals, John Wiley & Sons, Inc., Hoboken, NJ, USA, 2014, pp. 98–133, https://doi.org/10.1002/9781118788301, ch4.

[46] M.L. McCrea-Hendrick, M. Bursch, K.L. Gullett, L.R. Maurer, J.C. Fettinger, S. Grimme, P.P. Power, Counterintuitive interligand angles in the diaryls E{C_6H_3-2,6-(C_6H_2-2,4,6-*i*Pr_3)$_2$}$_2$ (E = Ge, Sn, or Pb) and related species: the role of London dispersion forces, Organometallics 37 (2018) 2075–2085, https://doi.org/10.1021/acs.organomet.8b00225.

[47] G.H. Spikes, Y. Peng, J.C. Fettinger, P.P. Power, Synthesis and characterization of the monomeric sterically encumbered diaryls E{C_6H_3-2,6-(C_6H_3-2,6-Pr^i_2)$_2$}$_2$ (E = Ge, Sn, or Pb), Z. Anorg. Allg. Chem. 632 (2006) 1005–1010, https://doi.org/10.1002/zaac.200500532.

[48] K.K. Pandey, Relativistic DFT calculations of structure and ^{119}Sn NMR chemical shifts for bent M Sn C bonding in Power's metallostannylenes of chromium, molybdenum, tungsten and iron and diaryl stannylenes, J. Organomet. Chem. 815–816 (2016) 23–34, https://doi.org/10.1016/j.jorganchem.2016.05.006.

[49] P. Pyykkö, M. Atsumi, Molecular single-bond covalent radii for elements 1-118, Chem. Eur. J. 15 (2009) 186–197, https://doi.org/10.1002/chem.200800987.